FULL PAPER

BJC

British Journal of Cancer (2014) 111, 68–77 | doi: 10.1038/bjc.2014.282

Keywords: angiogenesis; antiangiogenic therapy; FGF-2; decoy receptor fusion protein; cancer therapy

A novel decoy receptor fusion protein for FGF-2 potently inhibits tumour growth

D Li[1], X Wei[1], K Xie[1], K Chen[1], J Li[1] and J Fang*[,1]

[1]School of Life Sciences and Technology, Tongji University, 1239 Siping Road, Shanghai 200092, China

Background: Antiangiogenic therapies have been proven effective in cancer treatment. Fibroblast growth factor-2 (FGF-2) has been functionally implicated in tumour angiogenesis and is an important target of antiangiogenic therapies. The aim of this work was to develop a novel FGF-2 inhibitor for cancer therapy.

Methods: Eleven fusion proteins were developed by fusing various truncated extracellular regions of FGFR1 with the Fc region of IgG1. The optimal decoy receptor fusion protein with the highest binding affinity for FGF-2 was identified by an FGF-2-binding assay and its potential antitumour effects were investigated.

Results: We obtained a soluble decoy receptor fusion protein with the highest binding activity for FGF-2, named FGF-Trap. Fibroblast growth factor-Trap significantly abolished FGF-2-stimulated activation of FGF signalling as demonstrated by its suppression of FGF-2-mediated phosphorylation of Erk1/2 and Akt, upregulation of cyclins D1 and E and the increase in mRNA levels of vascular endothelial growth factor R1 and R2 (VEGFR1 and VEGFR2). Furthermore, FGF-Trap effectively suppressed FGF-2-induced proliferation and migration of human umbilical vein endothelial cells (HUVECs) *in vitro*. Most importantly, FGF-Trap potently inhibited tumour growth and angiogenesis in Caki-1 and A549 xenograft models *in vivo*.

Conclusions: Fibroblast growth factor-Trap potently inhibits tumour growth by blocking FGF-2 signalling pathways and could be an effective therapeutic agent for cancer patients.

The fibroblast growth factor (FGF) family comprises at least 23 members, which function through four-transmembrane tyrosine kinase receptors (FGFR1, FGFR2, FGFR3 and FGFR4) on the surface of target cells (Turner and Grose, 2010). Among the FGF family members, fibroblast growth factor-2 (FGF-2) is well characterised, bearing all typical features of the FGF family, and is regarded as a prototypic growth factor (Cronauer *et al*, 2003). Fibroblast growth factor-2 is an important proangiogenic growth factor that stimulates the growth, survival and migration of endothelial cells, and promotes the development and tumour angiogenesis of multiple cancer types, including kidney and lung cancers (Bremnes *et al*, 2006; Cenni *et al*, 2007). It has been shown that FGF-2 is overexpressed in multiple cancer types, including melanoma, prostate cancer, renal cell cancer and lung cancer (Turner and Grose, 2010; Lieu *et al*, 2011; Welti *et al*, 2011). Fibroblast growth factor-2 expression levels were significantly higher in renal and lung cancer patients and were correlated to tumour progression and poor prognosis (Slaton *et al*, 2001; Joensuu *et al*, 2002; Kuhn *et al*, 2004; Horstmann *et al*, 2005). Additionally, among the multiple mechanisms of tumour resistance to anti-VEGF(R) therapies, the presence of activated alternative growth factors, such as FGF-2, in naive tumour or compensatory increase of these factors during the course of therapy might cause intrinsic or acquired resistance to anti-VEGF(R) therapies, respectively (Bergers and Hanahan, 2008; Reynolds, 2009; Sennino and McDonald, 2012; Vasudev and Reynolds, 2014). Indeed, FGF-2 has been reported to promote tumour angiogenesis independently of vascular endothelial growth factor (VEGF) (Cao *et al*, 2008) and mediate tumour resistance to anti-VEGF therapy (Welti *et al*, 2011). Experimental evidence has shown that tumour growth can be restimulated by the compensatory upregulation of FGF-2 in late-stage pancreatic islet carcinoma

*Correspondence: Dr J Fang; E-mail: jfang@tongji.edu.cn

Received 17 February 2014; revised 29 April 2014; accepted 30 April 2014; published online 29 May 2014

undergoing anti-VEGFR2 treatment, which could be significantly diminished by adding an adenovirus-delivered soluble FGFR2 (Casanovas *et al*, 2005). Moreover, a recent study demonstrated that FGF-2 was responsible for the acquired resistance of head and neck squamous cell carcinoma to bevacizumab, an anti-VEGF monoclonal antibody. Treatment with an FGFR inhibitor, which blocks FGF-2 signalling resulted in a significant decrease in bevacizumab-resistant tumour growth (Gyanchandani *et al*, 2013). In a bevacizumab-resistant lung cancer xenograft model, the levels of circulating FGF-2 were significantly elevated in the plasma of mice (Cascone *et al*, 2011). Clinically, plasma levels of FGF-2 have also been found to increase significantly in parallel with tumour progression in recurrent glioblastoma patients and in metastatic colorectal cancer patients, as well as in renal cell carcinoma patients treated with anti-VEGF(R) agents (Batchelor *et al*, 2007; Cenni *et al*, 2007; Kopetz *et al*, 2010; Porta *et al*, 2013; Sharpe *et al*, 2013). These findings highlight the role of FGF-2 in tumour progression and in mediating resistance to anti-VEGF(R) therapies.

Currently, targeting FGF-2 signalling is an important strategy for anticancer drug development with various modules already under development, and with numerous anti-FGF-2 signalling agents in both preclinical and clinical trials. These include a variety of small-molecule receptor tyrosine kinase inhibitors, such as dovitinib (Andre *et al*, 2013) and nintedanib (Hilberg *et al*, 2008), as well as protein antiangiogenic agents, such as monoclonal antibodies (Tao *et al*, 2010; Wang *et al*, 2012) and chimeric soluble decoy receptor fusion proteins (Compagni *et al*, 2000; Harding *et al*, 2013). Given the side effects of small-molecular compounds and the potential immunogenic responses of murine antibodies, soluble decoy receptor fusion proteins might offer the most effective approach for blocking specific signalling pathways. So far, the best-studied protein antiangiogenic agent targeting the FGF pathway is FP-1039, a soluble decoy receptor fusion protein composed of the full-length FGFR1 extracellular region and the human IgG1 Fc fragment (Harding *et al*, 2013), which is currently in a phase II clinical trial (Brooks *et al*, 2012).

The binding affinity of a receptor extracellular domain to its specific ligand is critical when developing soluble decoy receptor fusion proteins. The extracellular region of FGFRs consists of three immunoglobulin-like domains (D1–D3) and a serine-rich region (termed the acid box), which is present in the D1–D2 linker. Alternative splicing of FGFR1–3 D3 yields two major isoforms, designated IIIb and IIIc. Fibroblast growth factor-2 binds with high affinity to the IIIc variant as determined by mitogenic stimulation, especially FGFR1 IIIc (Powers *et al*, 2000). FP-1039 has been proven to be effective in treating multiple types of cancer in preclinical studies (Harding *et al*, 2013). However, several studies have shown that both the D1 and the D1–D2 linker of FGFRs has an autoinhibitory role in ligand-receptor binding owing to the flexible nature of the D1–D2 linker region, which enables D1 to interact with the D2–D3 fragment of FGFR and affect the interaction with FGF and heparin (Wang *et al*, 1995; Olsen *et al*, 2004). These findings indicate that FP-1039 is not in the optimal composition to inhibit potently FGF-2. Moreover, the extracellular region of FGFR1 that is responsible for the highest binding affinity to FGF-2 has not yet been identified.

Taking into account the autoinhibition mechanism of FGFRs, we developed a series of soluble decoy receptor fusion proteins in the present study by fusing various truncated extracellular region of FGFR1 IIIc with the human IgG1 Fc fragment. One variant decoy receptor fusion protein, which we designated FGF-Trap, showed the highest affinity for FGF-2. Importantly, FGF-Trap potently inhibited the FGF signalling pathway and effectively suppressed FGF-2-induced cell proliferation and migration of human umbilical vein endothelial cells (HUVECs) *in vitro*, and significantly reduced the angiogenesis and tumour growth in two xenograft models *in vivo*.

MATERIALS AND METHODS

Cell lines and animals. Cells were maintained in a humidified incubator at 37 °C with 5% CO_2. Chinese hamster ovary (CHO) DG44 cells with dihydrofolate reductase (dhfr) deficiency were obtained from Life Technologies (Gaithersburg, MD, USA) and maintained in IMDM medium supplemented with 10% FBS and 1% hypoxanthine-thymidine (HT) (all from Life Technologies). Human umbilical vein endothelial cells were purchased from AllCells (Emeryville, CA, USA) and cultured in complete HUVEC medium (AllCells) containing 10% FBS and 10% growth factor supplement (AllCells). Caki-1 and A549 tumour cells were purchased from the Cell Bank of the Chinese Academy of Sciences (Shanghai, China) and propagated in DMEM medium (Life Technologies) supplemented with 10% FBS. All cells were characterised for DNA profiling, isoenzyme activity, vitality and mycoplasma contamination by the supplier, and were passaged for fewer than 6 months after receipt.

Female BALB/c nude mice (6–8 weeks old) were purchased from Shanghai SLRC Laboratory Animal (Shanghai, China) and housed under specific pathogen-free conditions with free access to food and water in the animal facility of Tongji University. The protocols were approved by the Animal Care and Use committee of Tongji University. All animal studies were carried out in accordance with institutional guidelines (Workman *et al*, 2010).

Construction of recombinant expression vectors. The gene sequences encoding the full-length extracellular region or truncated extracellular region of human FGFR1 were amplified by polymerase chain reaction (PCR) using commercial PCR Ready First Strand cDNA (BioChain, Hayward, CA, USA) as the template, fused with the Fc region of human IgG1, and then subcloned into a expression vector at the downstream of a CMV promoter. This plasmid also contains an open reading frame for DHFR driven by an SV40 promoter. All fusion proteins were preceded with a VEGFR1 signal peptide for secretion. Recombinant proteins were designated as FGF-Trap-1 to -10 according to the length of the extracellular region of FGFR1. Fibroblast growth factor-Trap-11 was constructed by removing the heparin binding site (HBS) on the basis of FGF-Trap-6.

Expression and purification of decoy receptor fusion proteins. Transfection of plasmid DNA was performed with the FuGENE HD transfection reagent (3 : 1 reagent to DNA ratio; Roche, Basel, Switzerland) in ~80% confluent CHO cells. Conditioned media were collected 48 h after transfection. The concentration of transiently expressed proteins was quantified by using a human IgG ELISA Quantitation Kit (Bethyl Laboratories, Montgomery, TX, USA), after which the protein samples were stored at −20 °C for later binding analysis. Stable transfected cells were selected in medium without HT, followed by isolation of single-cell clones by limiting dilution. Gene amplification was induced by gradient addition of methotrexate (from 10 to 500 nM; Sigma-Aldrich, St Louis, MO, USA). The decoy receptor fusion protein secreted into the medium was purified by Protein A affinity chromatography and anion exchange chromatography (GE Healthcare, Piscataway, NJ, USA) according to the manufacturer's instructions. The quality of FGF-Trap was determined by SDS–PAGE and the protein concentration was determined using the Lowry assay. The protein was reconstituted in sterile PBS and stored at −80 °C until use.

FGF-Trap-binding activity assay. Fibroblast growth factor-2-binding activity was assayed using ELISA. Briefly, 100 ng ml^{-1} of transiently expressed FGF-Traps were incubated with 50 ng ml^{-1} FGF-2 (R&D Systems, Minneapolis, MN, USA) in the presence or absence of 100 ng ml^{-1} heparin (Sigma-Aldrich) on immobilised plates for 1 h at room temperature. Plates were washed, incubated

with an HRP-conjugated goat anti-human IgG-Fc antibody (Bethyl Laboratories), washed again and treated with HRP substrate. Colour development was read at 450 nm using a spectrophotometer.

FGF-Trap-binding affinity assay. Binding affinity of the optimal FGF-Trap (i.e., FGF-Trap-6) for FGF-2 was determined using the Quantikine Human FGF-2 Immunoassay Kit (R&D Systems). Plates were precoated with a capture monoclonal antibody specific for FGF-2. Fibroblast growth factor-2 (20 pM) was mixed with an equal volume of FGF-Trap (ranging in concentration from 2×10^{-5} to 2×10^{3} pM) overnight at room temperature. To determine quantitatively the amount of unbound FGF-2 in the mixtures, standards and samples were added into the precoated plates and incubated at 37 °C for 2 h. Plates were washed, incubated with biotin-conjugated detection antibody and detected using streptavidin–HRP conjugate and peroxidase substrate. The colour changes were measured spectrophotometrically at 450 nm. The FGF-2 concentration in each sample was interpolated from a standard curve.

Cell proliferation and migration assays. For the HUVEC proliferation assay, HUVECs (3×10^{3} cells per well) were plated on 96-well plates and cultured overnight at 37 °C. The next day, purified FGF-Trap (from 0.128 to 10 000 ng ml^{-1}) mixed with 5 ng ml^{-1} FGF-2 in HUVEC basic medium (AllCells) containing 1% FBS (HBM) was added to the cells. For tumour cell proliferation assay, Caki-1 and A549 cells (2×10^{3} cells per well) were plated on 96-well plates and cultured overnight. The next day, purified FGF-Trap (from 0.64 to 50 000 ng ml^{-1}) diluted by 1% FBS medium was added to the cells. After incubation at 37 °C for 3–4 days, 10% (vol vol^{-1}) Cell Counting Kit-8 (CCK-8; Dojindo, Kumamoto, Japan) reagent was added into each well and incubated for an additional 4 h. The plate was read in a spectrophotometer at 450 nm.

For the HUVEC migration assay, HUVECs (5×10^{4} cells per well) were seeded in the upper chambers of transwell polycarbonate filters (Corning Costar, Cambridge, MA, USA) with 8 μm pores in the presence of FGF-Trap at various concentrations (0, 5, 50 and 500 ng ml^{-1}) in HBM. The filters were placed in the wells containing 10 ng ml^{-1} FGF-2 in HBM. After incubation for 16–24 h at 37 °C, the filters were removed and the cells on the upper surface were scraped with a cotton swab. The cells on the lower surface of the filter membrane were fixed in 100% methanol and stained with crystal violet (Sigma-Aldrich). The cells were counted in five random fields for each membrane using an Eclipse Ti inverted microscope (Nikon, Kanagawa, Japan) at × 200 magnification.

Western blot and quantitative real-time PCR. For the signalling assay, HUVECs (10^{5} cells per well) were seeded in 12-well plates in HBM overnight, and then treated with 10 ng ml^{-1} FGF-2 and/or 5 μg ml^{-1} FGF-Trap for 10 min. The cells were subsequently lysed on ice in RIPA buffer, after which total proteins were extracted for western blotting with the following specific antibodies: anti-p-Erk1/2, anti-Erk1/2, anti-p-Akt or anti-Akt (Cell Signaling Technology, Beverly, MA, USA). Similarly, 3 days after treatment with 20 ng ml^{-1} FGF-2 and/or 10 μg ml^{-1} FGF-Trap, cells were lysed for immunoblotting of cyclin D1, cyclin-E (Santa Cruz Biotechnology, Santa Cruz, CA, USA) and GAPDH (Cell Signaling Technology) as a loading control. Densitometric analysis of western blots was performed with Image-Pro Plus 6.0 software (Media Cybernetics, Silver Spring, MD, USA). Total RNA of HUVECs was extracted after treatment with FGF-2 and/or FGF-Trap for 3 days and reverse-transcribed to cDNA for quantitative real-time PCR (qPCR) as described previously (Li *et al*, 2014) using the published primers for VEGFR1, VEGFR2 and β-actin (Chung *et al*, 2004).

Pharmacokinetic analysis. Blood samples of female BALB/c nude mice were collected at 1, 2, 8, 24, 48, 72, 120, 168, 288, 360 and 504 h after a single intraperitoneal injection of 100 μg FGF-Trap ($n = 10$, five mice per time point). The concentration of serum FGF-Trap was measured by using the human IgG ELISA Quantitation Kit (Bethyl Laboratories).

Tumour xenograft models. Caki-1 cells (2×10^{6} cells per mouse) and A549 cells (5×10^{6} cells per mouse) were suspended in serum-free DMEM medium and subcutaneously injected into the right flanks of female BALB/c nude mice. Tumour size was monitored two times a week with a calipre and tumour volume was calculated by the following formula: tumour volume (mm^3) = length × width × width/2. When tumour size reached around 50 mm^3, animals were randomised into four groups, which received an intraperitoneal injection of FGF-Trap at a dose of 25, 2.5 and 0.25 mg kg^{-1} or PBS vehicle two times weekly for 5 to 7 weeks ($n = 7$–8 per group).

Histology and immunofluorescence analysis. Three days after the last dose, mice were killed and the tumour tissues were excised and fixed in 4% paraformaldehyde overnight. Following paraffin embedding, tissues were sectioned at 8 μm thinkness and stained using a Haematoxylin and Eosin Staining Kit (Beyotime Institute of Biotechnology, Jiangsu, China) for microscopic observation at × 200 magnification. For immunofluorecsence staining, sections were dewaxed and antigen retrieved with citrate buffer (pH 6.0) at 95 °C for 20 min. Subsequently, sections were blocked with 5% BSA at 37 °C for 10 min and incubated with goat anti-mouse CD34 antibody (Boster, Wuhan, China) at 4 °C overnight. Following washes in PBS, Cy3-conjugated rabbit anti-goat IgG secondary antibody (Boster) was applied at 37 °C for 1 h. Nuclei were stained with 4′-6-diamidino-2-phenylindole (DAPI) at 37 °C for 5 min, after which the sections were mounted using antifade fluorescent mounting medium (Boster). Fluorescence was evaluated using a Leica TCS SP5 II confocal laser scanning microscope (Leica Microsystems, Wetzlar, Germany). The number of tumour nuclei per high-power field and the percentage of CD34^{+} areas per field were quantified as described previously (Martens *et al*, 2006; Xue *et al*, 2008) using Image-Pro Plus 6.0 software (Media Cybernetics).

Statistical analyses. Graphs were constructed using GraphPad Prism (Graphpad Software, San Diego, CA, USA). All data are presented as mean ± s.e.m. Statistical significance was determined by unpaired two-tailed *t*-tests or two-way ANOVAs. $P < 0.05$ was considered statistically significant.

RESULTS

Deletion of the N-terminal 144-amino-acid residues results in the highest binding affinity of decoy receptor fusion protein to FGF-2. To investigate the influence of the D1 and D1–D2 linker of FGFR1 on the binding activity for FGF-2, we transiently expressed a series of recombinant FGF-Traps containing full-length extracellular regions or truncated extracellular regions of FGFR1c (GenBank accession no. NM_015850). The amino-acid sequences of FGFR1 portions included in FGF-Traps (from FGF-Trap-1 to FGF-Trap-10) were amino acids (aa) 22–374, 77–374, 102–374, 134–374, 142–374, 145–374, 146–374, 148-374, 151–374 and 156–374, respectively. Fibroblast growth factor-Trap-11 was created by removing the HBS (aa 158–175) on the basis of FGF-Trap-6. The schematic representation of the structure of various FGF-Traps is shown in Figure 1A.

To test the binding affinity of FGF-Traps for FGF-2, FGF-Traps were incubated with FGF-2 in the presence or absence of heparin, followed by the addition of HRP-conjugated goat anti-human IgG-Fc antibody and HRP substrate. The formation of

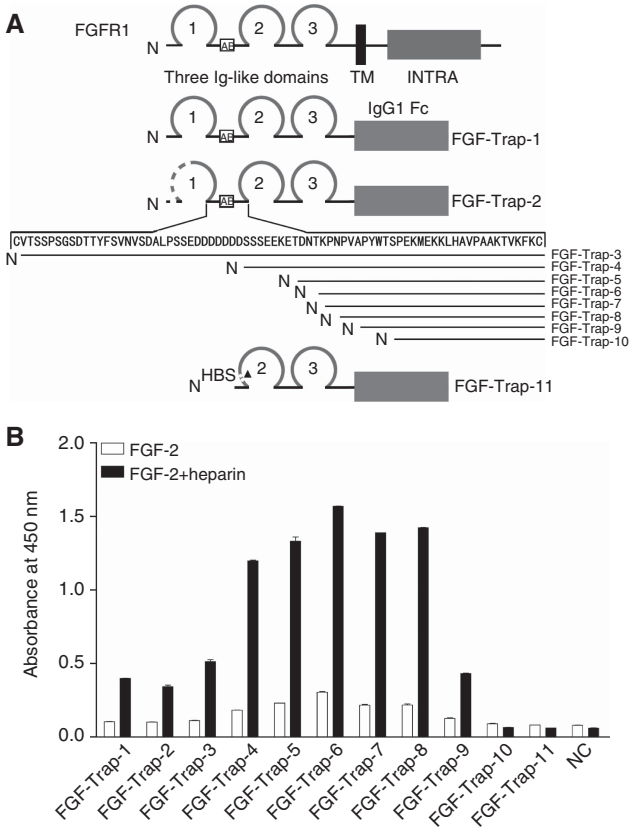

Figure 1. Engineering and binding activity of decoy receptor fusion proteins. (**A**) Engineering of decoy receptor fusion proteins. Multiple extracellular domains of FGFR1 were fused with the Fc portion of human IgG1. Amino terminus of various proteins is shown as N, whereas the transmembrane domain (TM), intracellular domain (INTRA) and IgG1 Fc are indicated by solid rectangles. Ig-like domains are shown as loops; 1–3 indicates the number of respective Ig-like domains. The amino-acid residues of the D1–D2 linker are indicated by arrows. The acidic box is shown as AB within the open box. Dotted lines indicate sequence deletions and the heparin binding site is shown as HBS. (**B**) Binding activity of decoy receptor fusion proteins. The 96-well plates were precoated with 50 ng ml^{-1} FGF-2 in the absence (open squares) or presence (filled squares) of 100 ng ml^{-1} heparin at 4 °C overnight, after which conditioned media from CHO cells either as a negative control (NC) or containing 100 ng ml^{-1} decoy receptor fusion protein was added and followed by incubation with a horse radish peroxidase (HRP)-conjugated secondary antibody. The resulting absorbance was detected at 450 nm after adding HRP substrate and stop solution. The colour reproduction of this figure is available on the *British Journal of Cancer* journal online.

FGF-Trap/FGF-2 complex was measured by the colour development catalysed by HRP. The results showed that heparin significantly increased the binding of FGF-Traps to FGF-2. Interestingly, we found that gradual deletion of the N-terminus amino-acid residues 22–to 144 (FGF-Trap-1 to FGF-Trap-6) increased the binding activity of FGF-Traps (Figure 1B). However, further deletion of N-terminus amino-acid residues on the basis of FGF-Trap-6 decreased the binding activity of FGF-Traps (Figure 1B). In particular, FGF-Trap-10, which was 11-amino-acid residues less than FGF-Trap-6, almost completely lost its binding activity (Figure 1B). To investigate the role of the HBS, the HBS sequence was deleted from FGF-Trap-6 to yield FGF-Trap-11. We found that FGF-Trap-11 could not bind FGF-2 (Figure 1B). These data demonstrate that HBS is essential for the formation of an FGF-2:FGF-Trap:heparin ternary complex and that deletion of the N-terminal 144-amino-acid residues results in the highest binding affinity of FGF-Trap for FGF-2. Given these findings, we chose FGF-Trap-6 as the optimal decoy receptor fusion protein for FGF-2, hereafter referred to as FGF-Trap (Figure 2A).

Characterisation of FGF-Trap. Fibroblast growth factor-Trap was highly purified from conditioned media of stably transfected cells by combined purification procedures. The structure of FGF-Trap is shown in Figure 2A. The purity and the molecular weight of FGF-Trap were determined by non-reducing (Figure 2B) and reducing SDS–PAGE (Figure 2C), respectively. We detected only a single band in each lane of each gel, with purity $>$ 98%. As FGF-Trap has eight potential N-glycosylation sites based on the Asn-X-Thr/Ser consensus sequence, this resulted in an increased molecular weight in comparison with the theoretical value of 102.4 kDa. Results of the binding affinity assay showed that FGF-Trap displayed a K_d of approximately 1.4×10^{-3} pM (Figure 2D). To examine the pharmacokinetic properties of FGF-Trap, FGF-Trap was intraperitoneally injected into BALB/c nude mice. Serum FGF-Trap concentration was measured at the indicated time points. The results showed that FGF-Trap had high pharmacokinetic properties, with a maximal concentration (C_{max}) of 97.7 μg ml^{-1} and total area under the curve concentration of 621 μg $\times$ days per ml (Figure 2E).

FGF-Trap inhibits the proliferation and migration of HUVECs, and the proliferation of tumour cells. To determine the activity of FGF-Trap in inhibiting FGF-2-induced cell proliferation, we treated HUVECs with serially diluted FGF-Trap in the presence of FGF-2 and measured cell proliferation by CCK-8 with HUVECs without treatment as a negative control. Fibroblast growth factor-Trap significantly suppressed FGF-2-induced cell proliferation in a concentration-dependent manner with an IC_{50} of 0.066 μg ml^{-1} (Figure 3A). We additionally measured the activity of FGF-Trap in blocking FGF-2-induced HUVEC cell migration by using a transwell chamber migration assay system. We found that FGF-2 stimulated the migration of HUVECs (Figures 3B and C), which was significantly attenuated by treatment with FGF-Trap at concentrations of 5, 50 and 500 ng ml^{-1}, respectively, yielding an inhibition rate of 12.9%, 22.2% and 77.8%, respectively. This demonstrated that FGF-Trap efficiently blocks FGF-2 signalling in the promotion of cell proliferation and migration.

We also assessed the direct effect of FGF-Trap on the proliferation of Caki-1 and A549 tumour cells. Fibroblast growth factor-Trap moderately inhibited the proliferation of these two tumour cells, with approximately 30% inhibition rate at 50 μg ml^{-1} FGF-Trap (Figure 3D). These results support the previous studies, which demonstrated that FGF signalling is important for the growth of some cancer cell lines and FGF-2 inhibitors have antitumour activity *in vitro* (Tao *et al*, 2010; Sharpe *et al*, 2011; Wang *et al*, 2012).

FGF-Trap suppresses FGF-2-mediated phosphorylation of Erk1/2 and Akt, upregulation of cyclins D1 and E and increase of the mRNA levels of VEGFR1 and VEGFR2. To explore whether FGF-Trap suppresses FGF-2-mediated signalling pathways, we used immunoblotting to first determine the phosphorylation states of FGF-2 downstream signalling molecules Erk1/2 and Akt in HUVECs after treatment with FGF-2 and/or FGF-Trap. Fibroblast growth factor-2 activated the Erk1/2-MAPK and PI3K-Akt signalling pathways as demonstrated by the increased phosphorylation of Erk1/2 and Akt. In contrast, FGF-Trap suppressed FGF-2-stimulated phosphorylation of both Erk1/2 and Akt (Figures 4A–C). Another function of FGF-2 signalling is to promote cell cycle progression by increasing the expression of cyclins. Indeed, we found that FGF-2 upregulated the protein levels of both cyclins D1 and E in HUVECs, and that this was suppressed by FGF-Trap (Figures 4D–F). To test the effects of FGF-Trap on

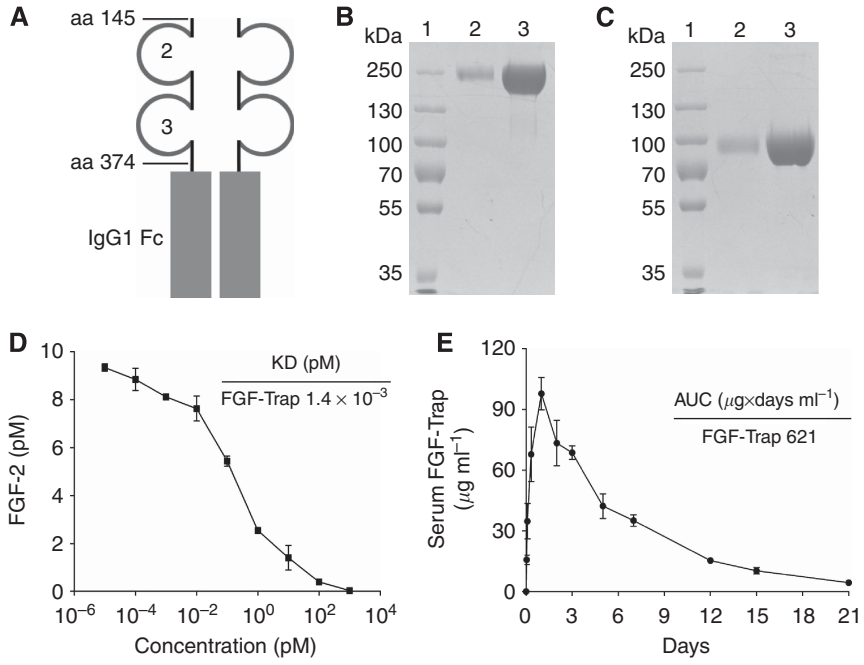

Figure 2. The structure and characterisation of FGF-Trap. (**A**) Schematic representation of the structure of FGF-Trap. (**B** and **C**) Sodium dodecyl sulphate–polyacrylamide gel electrophoresis (SDS–PAGE) analyses of FGF-Trap under non-reducing (**B**) and reducing (**C**) conditions. Lane 1, protein marker; lane 2, 1 μg FGF-Trap; lane 3, 10 μg FGF-Trap. (**D**) Binding affinity of FGF-Trap for FGF-2 was determined by incubation of FGF-Trap with 10 pM FGF-2. (**E**) Pharmacokinetic analysis of FGF-Trap. FGF-Trap of 100 μg was intraperitoneally injected into BALB/c nude mice, and blood was drawn at the indicated time points. The serum level of FGF-Trap was measured by enzyme-linked immunosorbent assay.
The colour reproduction of this figure is available on the *British Journal of Cancer* journal online.

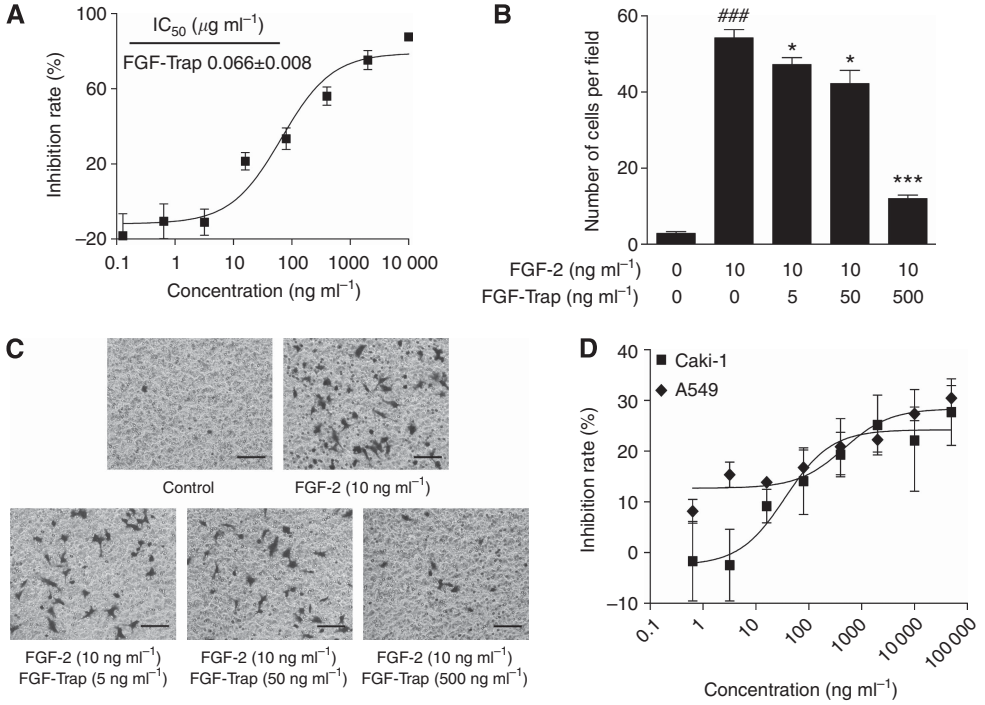

Figure 3. Fibroblast growth factor-Trap inhibits the proliferation and migration of vascular endothelium cells, and the proliferation of tumour cells *in vitro*. (**A**) Inhibition of FGF-2-induced HUVEC proliferation by FGF-Trap. Human umbilical vein endothelial cells were seeded in 96-well plates overnight and treated with FGF-Trap in the presence of FGF-2 for 3 days. The cell proliferation was determined by CCK-8 reagent. (**B** and **C**) Inhibition of FGF-2-induced HUVEC migration by FGF-Trap. After incubation, HUVECs migrated to the lower surface of the membrane as revealed by crystal violet staining. The number of migrated cells (**B**) was counted from five random fields for each membrane under a light microscope at $\times$200 magnification (**C**). $^{###}P<0.001$, compared with control; $^{*}P<0.05$, $^{***}P<0.001$, compared with FGF-2-treated group using unpaired, two-tailed *t*-tests. Scare bars, 100 μm. (**D**) Inhibition of Caki-1 and A549 tumour cell proliferation by FGF-Trap. Caki-1 and A549 cells were seeded in 96-well plates overnight, and treated with FGF-Trap for 4 days. The cell proliferation was determined by CCK-8 reagent.
The colour reproduction of this figure is available on the *British Journal of Cancer* journal online.

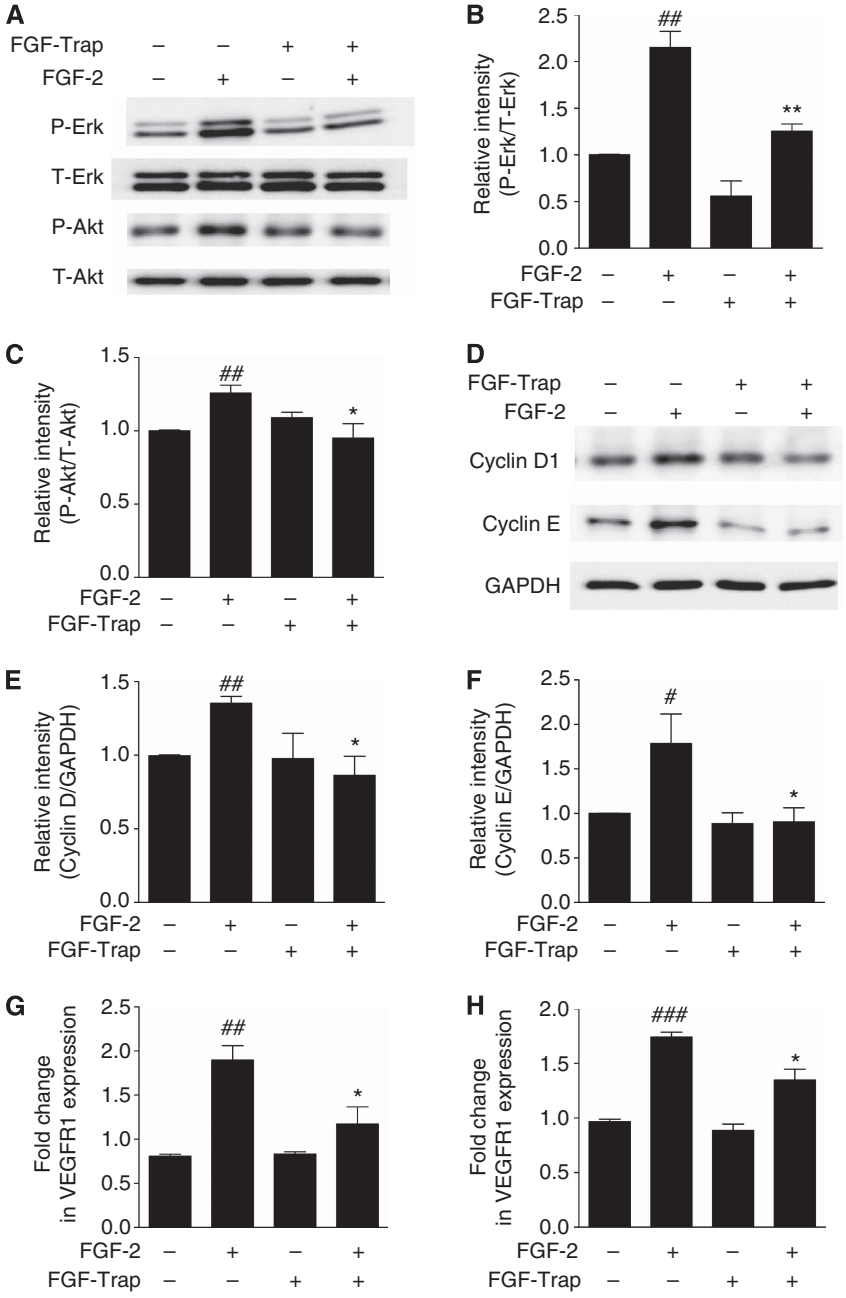

Figure 4. Fibroblast growth factor-Trap suppresses FGF-2-mediated signalling pathways, cell cycle progression and VEGFR mRNA expression. (**A**) Representative western blots of phosphorylated (P-Erk) and total Erk1/2 (T-Erk), phosphorylated (P-Akt) and total Akt (T-Akt) from HUVECs induced with or without FGF-2 (10 ng ml^{-1}) and FGF-Trap (5 μg ml^{-1}) for 10 min. (**B** and **C**) Quantitative results are illustrated for (**A**). Each column represents the density of the immunoreactive P-Erk band (**B**) normalised to the T-Erk band, and P-Akt band (**C**) normalised to the T-Akt band from a minimum of three independent assays. $^{\#\#}P<0.01$, compared with untreated cell; $^{*}P<0.05$, $^{**}P<0.01$, compared with FGF-2-treated cell using unpaired, two-tailed *t*-tests. (**D**) Representative western blots of cyclins D1 and E in HUVECs treated with or without FGF-2 (20 ng ml^{-1}) and FGF-Trap (10 μg ml^{-1}) for 3 days. Glyceraldehyde 3-phosphate dehydrogenase (GAPDH) was used as a protein loading control. (**E** and **F**) Quantitative results are illustrated for (**D**). Each column represents the density of the immunoreactive cyclin D1 band (**E**) and cyclin E band (**F**) normalised to the GAPDH band from a minimum of three independent assays, respectively. $^{\#\#}P<0.01$, compared with untreated cell; $^{*}P<0.05$, compared with FGF-2 treated cell using unpaired, two-tailed *t* tests. (**G** and **H**) Expression of VEGFR1 (**G**) and VEGFR2 (**H**) mRNA was quantified using qPCR. Changes in mRNA expression were expresses as fold change relative to β-actin ($n=3$). $^{\#\#}P<0.01$, $^{\#\#\#}P<0.001$, compared with untreated cell; $^{*}P<0.05$, compared with FGF-2 treated cell using unpaired, two-tailed *t*-tests.

FGF signalling-mediated angiogenesis, we further measured the mRNA expression of VEGFR1 and VEGFR2 by qPCR and found that both VEGFR1 (Figure 4G) and VEGFR2 (Figure 4H) mRNA expression levels were significantly increased after treatment with FGF-2, suggesting that in line with previously findings (Murakami *et al*, 2011; Saylor *et al*, 2012), there is a cross-talk between FGF(R) and VEGF(R). Intriguingly, FGF-Trap significantly suppressed FGF-2-mediated mRNA expression of VEGFR1 and VEGFR2 (Figures 4G and H).

FGF-Trap potently inhibits the tumour growth of mouse xenograft models. To evaluate the antitumour activity of

FGF-Trap *in vivo*, Caki-1 and A549 tumour cells were subcutaneously implanted into the right flanks of mice. After implantation, mice were allowed 1 week to form tumours, after which they received intraperitoneal injections of either 25, 2.5, 0.25 mg kg^{-1} FGF-Trap or vehicle two times weekly. Tumour volume and body weight of mice were also measured two times a week for 5–7 weeks (Figures 5A–D), after which mice were killed and tumours were excised and photographed (Figures 5E and F). The results showed that FGF-Trap significantly inhibited tumour growth in a dose-dependent manner. The potential toxicity of FGF-Trap was examined by comparing changes in body weight of mice among FGF-Trap and vehicle treatments. No significant differences were found when FGF-Trap used at does of up to 25 mg kg^{-1} (Figures 5C and D).

FGF-Trap inhibits tumour angiogenesis. To gain insight into the mechanism of antitumour properties of FGF-Trap *in vivo*, we performed histological and immunofluorescence studies on two xenograft tumour models. Haematoxylin and eosin staining of tumour sections showed that treatment of tumours with 25 mg kg^{-1} FGF-Trap resulted in numerous pyknotic/karyorrhectic nuclei and nuclear debris when compared with vehicle-treated tumours, indicative of degenerative cells undergoing apoptosis (Figures 6A and C). Quantification of nuclei in tumour sections from the 25 mg kg^{-1} FGF-Trap-treated group relative to the vehicle-treated group revealed a 67.2% reduction in Caki-1 tumours (Figure 6B) and 51.9% reduction in A549 tumours (Figure 6D). To further investigate the effects of FGF-Trap on inhibition of tumour angiogenesis, tumour sections were analysed by immunofluorescent staining of CD34, a marker of vascular endothelial cells (Pusztaszeri *et al*, 2006). Compared with vehicle-treated tumour tissues, an obvious reduction in blood vessels in 25 mg kg^{-1} FGF-Trap-treated Caki-1 and A549 tumour tissues was observed (Figures 6E and G). The number of CD34^{+} cells in the two models under FGF-Trap treatment was significantly lower than that of vehicle-treated group (Figures 6F and H). Collectively, these results demonstrated that the antitumour activity of FGF-Trap is mediated at least in part by inhibition of tumour angiogenesis.

DISCUSSION

In this study, we identified and subsequently engineered a novel decoy receptor fusion protein FGF-Trap with the highest binding affinity for FGF-2 by serial deletion of the amino terminus of FGFR1c. Fibroblast growth factor-Trap effectively inhibited the FGF-2 signalling pathway and inhibited the proliferation and migration of endothelial cells *in vitro*. Most importantly, FGF-Trap potently suppressed the angiogenesis and growth of mouse tumour xenografts *in vivo*. Our study suggests that targeting the FGF/FGFR signalling axis by soluble decoy receptor fusion proteins is a promising strategy for cancer therapy.

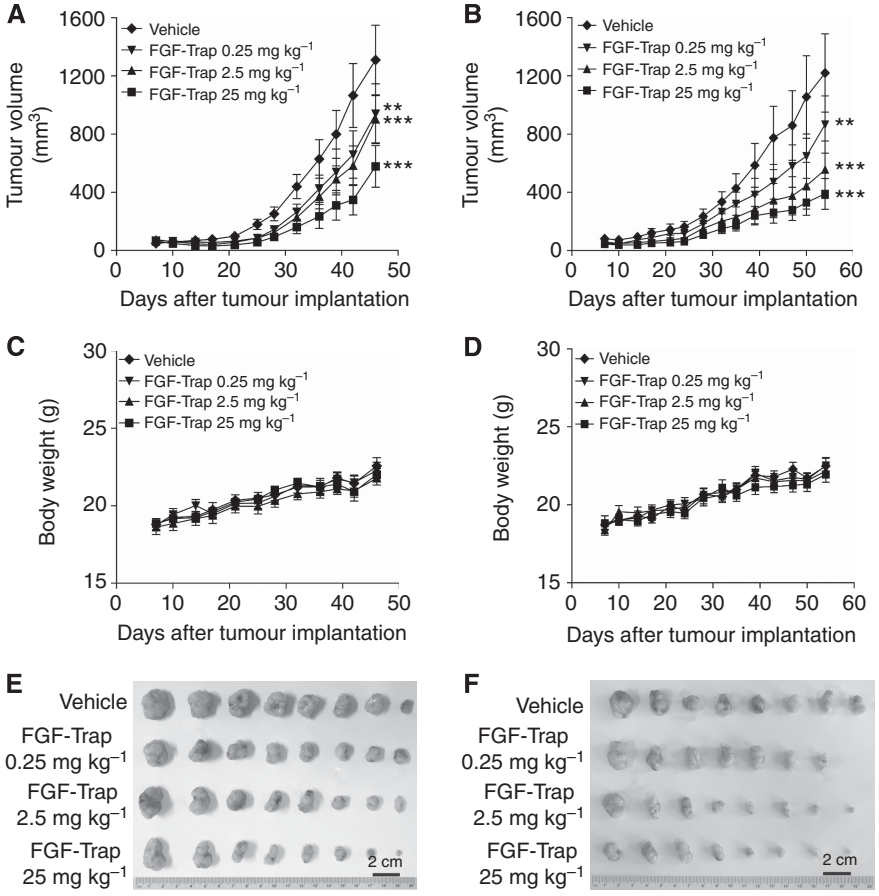

Figure 5. Fibroblast growth factor-Trap inhibits the growth of tumours *in vivo*. (**A**–**D**) Effects of FGF-Trap on tumour growth and body weight of mice. A total of 2×10^6 Caki-1 cells per mouse (**A** and **C**) and 5×10^6 A549 cells per mouse (**B** and **D**) were subcutaneously injected into the right flank of BALB/c nude mice. One week after implantation, mice received intraperitoneal injection of 25, 2.5 and 0.25 mg kg^{-1} FGF-Trap or vehicle two times weekly for 5–7 weeks, after which tumour volume (**A** and **B**) and body weight of mice (**C** and **D**) were measured ($n = 7$–8 per group). $^{**}P < 0.01$, $^{***}P < 0.001$, compared with vehicle group, two-way analysis of variance (ANOVA). (**E** and **F**) Photograph of the tumours. After 6–8 weeks of implantation, Caki-1 tumour-bearing mice (**E**) and A549 tumour-bearing mice (**F**) were killed and the tumours excised and photographed. The colour reproduction of this figure is available on the *British Journal of Cancer* journal online.

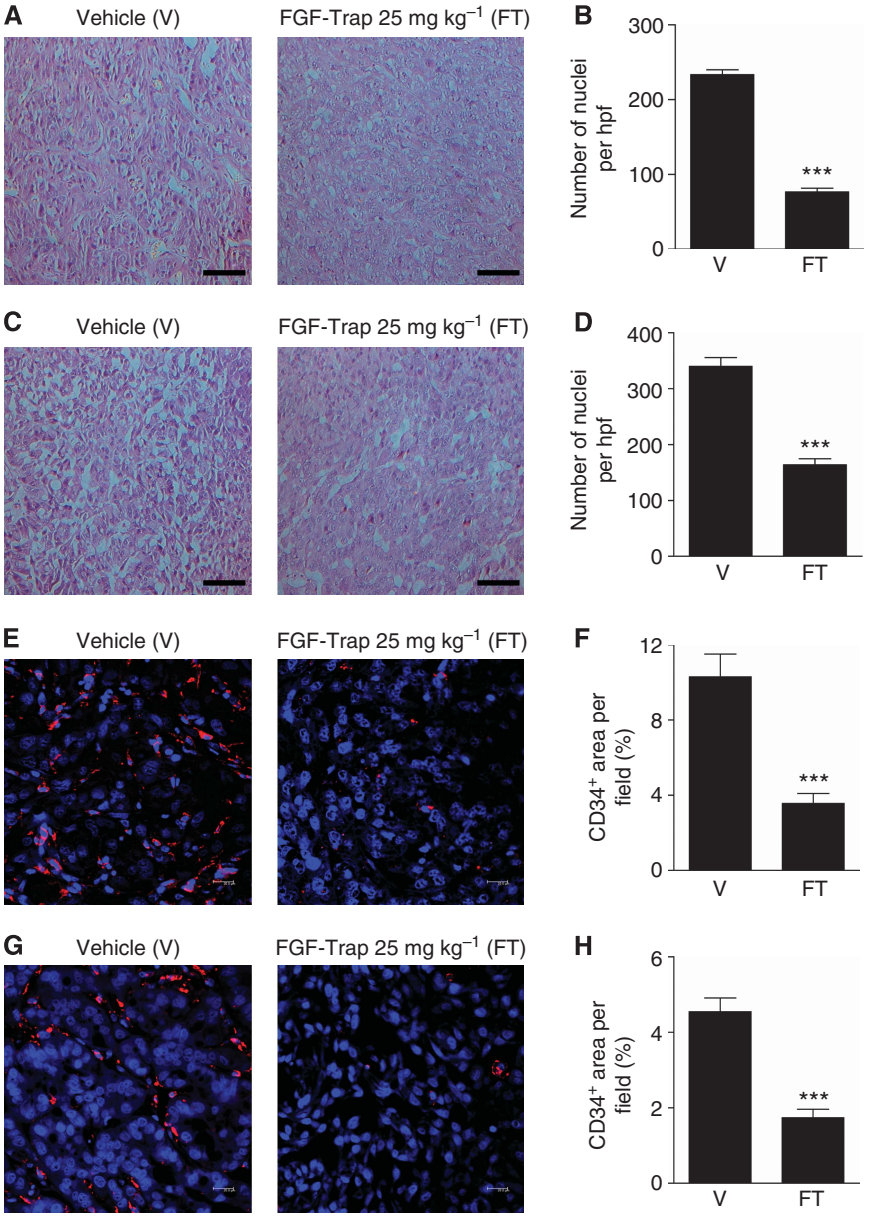

Figure 6. Histological and immunofluorescent analyses of tumour tissues. (**A–D**) Representative images of H&E-stained Caki-1 (**A**) and A549 (**C**) tissue sections at × 200 magnification and the quantified number of Caki-1 (**B**) and A549 (**D**) nuclei in each section ($n = 5$). Scare bars, 100 μm. ***$P < 0.001$, unpaired, two-tailed *t*-test. (**E–H**) Representative images and quantification of immunofluorescence staining. Caki-1 (**E**) and A549 (**G**) tumour tissue sections were stained by anti-CD34 antibody, followed by a Cy3-conjugated secondary antibody (red) and a nuclear DAPI (blue) stain, and were observed using confocal laser scanning microscopy (× 63 magnification). Scare bars, 20 μm. CD34-positive area in Caki-1 sections (**F**) and A549 sections (**H**) were measured ($n = 5$). ***$P < 0.001$, unpaired, two-tailed *t*-test.

Angiogenesis is a hallmark of cancer (Hanahan and Weinberg, 2011) and thus blocking proangiogenic factor(s)-induced angiogenesis is regarded as an effective strategy for cancer therapy. Among proangiogenic growth factors, FGF-2 represents one of the best-characterised factors that promote tumourigenesis via a number of mechanisms including tumour angiogenesis as well as metastasis through interaction with FGFRs, which leads to the activation of downstream signalling pathways (Dunn *et al*, 2000). In light of this, we found that preventing FGF-2 from binding to FGFRs by administration of soluble decoy receptor fusion proteins can serve as an effective therapeutic strategy.

The choice of high-affinity decoy receptors for the respective ligands is critical for the generation of decoy receptor fusion proteins. Among FGFRs, the alternatively spliced IIIc form of FGFR1 shows the highest affinity (Ornitz *et al*, 1996; Powers *et al*, 2000). More recently, one decoy receptor fusion protein, FP-1039, which was developed by fusing the whole extracellular region of FGFR1 with IgG1 Fc, has been shown to be effective in preclinical as well as clinical trials (Harding *et al*, 2013). However, studies have suggested that both the D1 domain and the D1–D2 linker of FGFRs have a role in receptor autoinhibition, whereas the D2 and D3 domains are necessary for ligand binding and specificity (Wang *et al*, 1995; Olsen *et al*, 2004; Kalinina *et al*, 2012). In consideration of the autoinhibition mechanism of FGFRs, we reasoned that the full-length extracellular region of FGFR1 would not likely yield an optimal decoy receptor. Our findings from this study support this hypothesis and are in line with the previous studies.

Solving of the crystal structure of the FGF-2:FGFR1 dimeric complex has been instrumental in determining the necessary FGFR1 residues that engage in the primary interaction site of FGF-2 and FGFR1 (Plotnikov *et al*, 1999). However, the FGFR1 construct used for the crystal structure did not contain the D1 or

the acid box, and thus could not be used to evaluate precisely the function of either D1 or the D1–D2 linker of FGFR1. To identify the fragment of FGFR1 extracellular region that has the highest binding affinity for FGF2, we constructed 10 decoy receptor fusion proteins containing variant extracellular regions of FGFR1 and the Fc region of IgG1, and transiently expressed them in CHO cells. The binding activity of these decoy receptor fusion proteins showed that heparin significantly increased the binding of decoy receptor fusion proteins for FGF-2 and D1 and that the acid box of FGFR1 acts as an autoinhibitor for the binding to FGF-2, which is consistent with previous studies (Wang *et al*, 1995; Olsen *et al*, 2004). Importantly, we identified FGF-Trap-6, which contains neither the whole extracellular region of FGFR1 (FGF-Trap-1) nor the D2–D3 region of FGFR1 (FGF-Trap-10), as the optimal decoy receptor fusion protein for FGF-2 binding. Because the binding activity of FGF-Trap-6 was completely lost when HBS was removed, this finding suggested that HBS is essential for the process of binding and is in line with the known role of heparin in FGFR binding and dimerisation (Schlessinger *et al*, 2000).

Among the FGF-Traps, FGF-Trap-10 was only 11 residues shorter than FGF-Trap-6, but exhibited almost no ligand binding activity. To investigate the role of the 11 residues in ligand binding, we performed a homology modelling of FGF-Trap-6 and FGF-Trap-10 using the Swiss-Model (http://swissmodel.expasy.org) based on the dimeric FGF-2:FGFR1 complex (PDB ID code 1CVS). Following the structure analysis using PyMOL (www.pymol.org), we found that an α-helix disappeared in the N terminus of FGF-Trap-10 when compared with FGF-Trap-6, indicating that the α-helix formation in the N-terminal region provides an energetic source for high affinity binding of FGF-Trap to FGF-2.

To explore the value of FGF-Trap as an anticancer therapeutic agent, we determined the capacity for FGF-Trap to suppress indices of tumour formation both *in vivo* and *ex vivo*. We chose Caki-1 and A549 cells in our study for three reasons. First, FGF-2 has important roles in regulating the development and tumour angiogenesis of kidney and lung cancers, as well as in tumour resistance to anti-VEGF(R) therapies (Cascone *et al*, 2011; Welti *et al*, 2011). Second, these tumour cell lines are human tumour cell lines with high level of FGF-2 expression (Takayama *et al*, 2000; Keyes *et al*, 2003; Kuhn *et al*, 2004). Third, these two tumour cell lines have high rate of tumour formation and have been widely used to assess the efficacy of antiangiogenic agents (Shi and Siemann, 2002; Yen *et al*, 2006; Huang *et al*, 2008; Kawada *et al*, 2014). Our findings showed that FGF-Trap proteins could significantly inhibit FGF-2-induced proliferation, migration and downstream signalling of HUVEC while they suppress the proliferation of tumour cells *in vitro* and the growth of tumours in mice in a dose-dependent manner.

Taken together, FGF-Trap is a novel soluble decoy receptor fusion protein that efficiently binds and blocks FGF-2, and may serve as a powerful therapeutic strategy for the treatment of cancer. Further studies are needed to evaluate the effects of FGF-Trap on tumour metastasis and acquired resistance to anti-VEGF therapy.

ACKNOWLEDGEMENTS

This work was supported by the Shanghai Committee of Science and Technology, China (12431901000 to JF). We are grateful to Hongwen Li and Xuejing Yao for experimental assistance.

CONFLICT OF INTEREST

The authors declare no conflict of interest.

REFERENCES

Andre F, Bachelot T, Campone M, Dalenc F, Perez-Garcia JM, Hurvitz SA, Turner N, Rugo H, Smith JW, Deudon S, Shi M, Zhang Y, Kay A, Porta DG, Yovine A, Baselga J (2013) Targeting FGFR with dovitinib (TKI258): preclinical and clinical data in breast cancer. *Clin Cancer Res* **19**(13): 3693–3702.

Batchelor TT, Sorensen AG, di Tomaso E, Zhang WT, Duda DG, Cohen KS, Kozak KR, Cahill DP, Chen PJ, Zhu M, Ancukiewicz M, Mrugala MM, Plotkin S, Drappatz J, Louis DN, Ivy P, Scadden DT, Benner T, Loeffler JS, Wen PY, Jain RK (2007) AZD2171, a pan-VEGF receptor tyrosine kinase inhibitor, normalizes tumor vasculature and alleviates edema in glioblastoma patients. *Cancer Cell* **11**(1): 83–95.

Bergers G, Hanahan D (2008) Modes of resistance to anti-angiogenic therapy. *Nat Rev Cancer* **8**(8): 592–603.

Bremnes RM, Camps C, Sirera R (2006) Angiogenesis in non-small cell lung cancer: the prognostic impact of neoangiogenesis and the cytokines VEGF and bFGF in tumours and blood. *Lung Cancer* **51**(2): 143–158.

Brooks AN, Kilgour E, Smith PD (2012) Molecular pathways: fibroblast growth factor signaling: a new therapeutic opportunity in cancer. *Clin Cancer Res* **18**(7): 1855–1862.

Cao Y, Cao R, Hedlund EM (2008) R regulation of tumor angiogenesis and metastasis by FGF and PDGF signaling pathways. *J Mol Med (Berl)* **86**(7): 785–789.

Casanovas O, Hicklin DJ, Bergers G, Hanahan D (2005) Drug resistance by evasion of antiangiogenic targeting of VEGF signaling in late-stage pancreatic islet tumors. *Cancer Cell* **8**(4): 299–309.

Cascone T, Herynk MH, Xu L, Du Z, Kadara H, Nilsson MB, Oborn CJ, Park YY, Erez B, Jacoby JJ, Lee JS, Lin HY, Ciardiello F, Herbst RS, Langley RR, Heymach JV (2011) Upregulated stromal EGFR and vascular remodeling in mouse xenograft models of angiogenesis inhibitor-resistant human lung adenocarcinoma. *J Clin Invest* **121**(4): 1313–1328.

Cenni E, Perut F, Granchi D, Avnet S, Amato I, Brandi ML, Giunti A, Baldini N (2007) Inhibition of angiogenesis via FGF-2 blockage in primitive and bone metastatic renal cell carcinoma. *Anticancer Res* **27**(1A): 315–319.

Chung JY, Song Y, Wang Y, Magness RR, Zheng J (2004) Differential expression of vascular endothelial growth factor (VEGF), endocrine gland derived-VEGF, and VEGF receptors in human placentas from normal and preeclamptic pregnancies. *J Clin Endocrinol Metab* **89**(5): 2484–2490.

Compagni A, Wilgenbus P, Impagnatiello MA, Cotten M, Christofori G (2000) Fibroblast growth factors are required for efficient tumor angiogenesis. *Cancer Res* **60**(24): 7163–7169.

Cronauer MV, Schulz WA, Seifert HH, Ackermann R, Burchardt M (2003) Fibroblast growth factors and their receptors in urological cancers: basic research and clinical implications. *Eur Urol* **43**(3): 309–319.

Dunn IF, Heese O, Black PM (2000) Growth factors in glioma angiogenesis: FGFs, PDGF, EGF, and TGFs. *J Neurooncol* **50**(1-2): 121–137.

Gyanchandani R, Ortega Alves MV, Myers JN, Kim S (2013) A proangiogenic signature is revealed in FGF-mediated bevacizumab-resistant head and neck squamous cell carcinoma. *Mol Cancer Res* **11**(12): 1585–1596.

Hanahan D, Weinberg RA (2011) Hallmarks of cancer: the next generation. *Cell* **144**(5): 646–674.

Harding TC, Long L, Palencia S, Zhang H, Sadra A, Hestir K, Patil N, Levin A, Hsu AW, Charych D, Brennan T, Zanghi J, Halenbeck R, Marshall SA, Qin M, Doberstein SK, Hollenbaugh D, Kavanaugh WM, Williams LT, Baker KP (2013) Blockade of nonhormonal fibroblast growth factors by FP-1039 inhibits growth of multiple types of cancer. *Sci Transl Med* **5**(178): 178ra39.

Hilberg F, Roth GJ, Krssak M, Kautschitsch S, Sommergruber W, Tontsch-Grunt U, Garin-Chesa P, Bader G, Zoephel A, Quant J, Heckel A, Rettig WJ (2008) BIBF 1120: triple angiokinase inhibitor with sustained receptor blockade and good antitumor efficacy. *Cancer Res* **68**(12): 4774–4782.

Horstmann M, Merseburger AS, von der Heyde E, Serth J, Wegener G, Mengel M, Feil G, Hennenlotter J, Nagele U, Anastasiadis A, Bokemeyer C, Stenzl A, Kuczyk M (2005) Correlation of bFGF expression in renal cell cancer with clinical and histopathological features by tissue microarray analysis and measurement of serum levels. *J Cancer Res Clin Oncol* **131**(11): 715–722.

Huang D, Ding Y, Luo WM, Bender S, Qian CN, Kort E, Zhang ZF, VandenBeldt K, Duesbery NS, Resau JH, Teh BT (2008) Inhibition of

MAPK kinase signaling pathways suppressed renal cell carcinoma growth and angiogenesis *in vivo*. *Cancer Res* **68**(1): 81–88.

Joensuu H, Anttonen A, Eriksson M, Makitaro R, Alfthan H, Kinnula V, Leppa S (2002) Soluble syndecan-1 and serum basic fibroblast growth factor are new prognostic factors in lung cancer. *Cancer Res* **62**(18): 5210–5217.

Kalinina J, Dutta K, Ilghari D, Beenken A, Goetz R, Eliseenkova AV, Cowburn D, Mohammadi M (2012) The alternatively spliced acid box region plays a key role in FGF receptor autoinhibition. *Structure* **20**(1): 77–88.

Kawada I, Hasina R, Arif Q, Mueller J, Smithberger E, Husain AN, Vokes EE, Salgia R (2014) Dramatic antitumor effects of the dual MET/RON small-molecule inhibitor LY2801653 in non-small cell lung cancer. *Cancer Res* **74**(3): 884–895.

Keyes KA, Mann L, Cox K, Treadway P, Iversen P, Chen YF, Teicher BA (2003) Circulating angiogenic growth factor levels in mice bearing human tumors using Luminex Multiplex technology. *Cancer Chemother Pharmacol* **51**(4): 321–327.

Kopetz S, Hoff PM, Morris JS, Wolff RA, Eng C, Glover KY, Adinin R, Overman MJ, Valero V, Wen S, Lieu C, Yan S, Tran HT, Ellis LM, Abbruzzese JL, Heymach JV (2010) Phase II trial of infusional fluorouracil, irinotecan, and bevacizumab for metastatic colorectal cancer: efficacy and circulating angiogenic biomarkers associated with therapeutic resistance. *J Clin Oncol* **28**(3): 453–459.

Kuhn H, Kopff C, Konrad J, Riedel A, Gessner C, Wirtz H (2004) Influence of basic fibroblast growth factor on the proliferation of non-small cell lung cancer cell lines. *Lung Cancer* **44**(2): 167–174.

Li D, Xie K, Ding G, Li J, Chen K, Li H, Qian J, Jiang C, Fang J (2014) Tumor resistance to anti-VEGF therapy through up-regulation of VEGF-C expression. *Cancer Lett* **346**(1): 45–52.

Lieu C, Heymach J, Overman M, Tran H, Kopetz S (2011) Beyond VEGF: inhibition of the fibroblast growth factor pathway and antiangiogenesis. *Clin Cancer Res* **17**(19): 6130–6139.

Martens T, Schmidt NO, Eckerich C, Fillbrandt R, Merchant M, Schwall R, Westphal M, Lamszus K (2006) A novel one-armed anti-c-Met antibody inhibits glioblastoma growth *in vivo*. *Clin Cancer Res* **12**(20 Pt 1): 6144–6152.

Murakami M, Nguyen LT, Hatanaka K, Schachterle W, Chen PY, Zhuang ZW, Black BL, Simons M (2011) FGF-dependent regulation of VEGF receptor 2 expression in mice. *J Clin Invest* **121**(7): 2668–2678.

Olsen SK, Ibrahimi OA, Raucci A, Zhang F, Eliseenkova AV, Yayon A, Basilico C, Linhardt RJ, Schlessinger J, Mohammadi M (2004) Insights into the molecular basis for fibroblast growth factor receptor autoinhibition and ligand-binding promiscuity. *Proc Natl Acad Sci USA* **101**(4): 935–940.

Ornitz DM, Xu J, Colvin JS, McEwen DG, MacArthur CA, Coulier F, Gao G, Goldfarb M (1996) Receptor specificity of the fibroblast growth factor family. *J Biol Chem* **271**(25): 15292–15297.

Plotnikov AN, Schlessinger J, Hubbard SR, Mohammadi M (1999) Structural basis for FGF receptor dimerization and activation. *Cell* **98**(5): 641–650.

Porta C, Paglino C, Imarisio I, Ganini C, Sacchi L, Quaglini S, Giunta V, De Amici M (2013) Changes in circulating pro-angiogenic cytokines, other than VEGF, before progression to sunitinib therapy in advanced renal cell carcinoma patients. *Oncology* **84**(2): 115–122.

Powers CJ, McLeskey SW, Wellstein A (2000) Fibroblast growth factors, their receptors and signaling. *Endocr Relat Cancer* **7**(3): 165–197.

Pusztaszeri MP, Seelentag W, Bosman FT (2006) Immunohistochemical expression of endothelial markers CD31, CD34, von Willebrand factor, and Fli-1 in normal human tissues. *J Histochem Cytochem* **54**(4): 385–395.

Reynolds AR (2009) Potential relevance of bell-shaped and u-shaped dose-responses for the therapeutic targeting of angiogenesis in cancer. *Dose Response* **8**(3): 253–284.

Saylor PJ, Escudier B, Michaelson MD (2012) Importance of fibroblast growth factor receptor in neovascularization and tumor escape from antiangiogenic therapy. *Clin Genitourin Cancer* **10**(2): 77–83.

Schlessinger J, Plotnikov AN, Ibrahimi OA, Eliseenkova AV, Yeh BK, Yayon A, Linhardt RJ, Mohammadi M (2000) Crystal structure of a ternary FGF–FGFR–heparin complex reveals a dual role for heparin in FGFR binding and dimerization. *Mol Cell* **6**(3): 743–750.

Sennino B, McDonald DM (2012) Controlling escape from angiogenesis inhibitors. *Nat Rev Cancer* **12**(10): 699–709.

Sharpe K, Stewart GD, Mackay A, Van Neste C, Rofe C, Berney D, Kayani I, Bex A, Wan E, O'Mahony FC, O'Donnell M, Chowdhury S, Doshi R, Ho-Yen C, Gerlinger M, Baker D, Smith N, Davies B, Sahdev A, Boleti E, De Meyer T, Van Criekinge W, Beltran L, Lu YJ, Harrison DJ, Reynolds AR, Powles T (2013) The effect of VEGF-targeted therapy on biomarker expression in sequential tissue from patients with metastatic clear cell renal cancer. *Clin Cancer Res* **19**(24): 6924–6934.

Sharpe R, Pearson A, Herrera-Abreu MT, Johnson D, Mackay A, Welti JC, Natrajan R, Reynolds AR, Reis-Filho JS, Ashworth A, Turner NC (2011) FGFR signaling promotes the growth of triple-negative and basal-like breast cancer cell lines both *in vitro* and *in vivo*. *Clin Cancer Res* **17**(16): 5275–5286.

Shi W, Siemann DW (2002) Inhibition of renal cell carcinoma angiogenesis and growth by antisense oligonucleotides targeting vascular endothelial growth factor. *Br J Cancer* **87**(1): 119–126.

Slaton JW, Inoue K, Perrotte P, El-Naggar AK, Swanson DA, Fidler IJ, Dinney CP (2001) Expression levels of genes that regulate metastasis and angiogenesis correlate with advanced pathological stage of renal cell carcinoma. *Am J Pathol* **158**(2): 735–743.

Takayama K, Ueno H, Nakanishi Y, Sakamoto T, Inoue K, Shimizu K, Oohashi H, Hara N (2000) Suppression of tumor angiogenesis and growth by gene transfer of a soluble form of vascular endothelial growth factor receptor into a remote organ. *Cancer Res* **60**(8): 2169–2177.

Tao J, Xiang JJ, Li D, Deng N, Wang H, Gong YP (2010) Selection and characterization of a human neutralizing antibody to human fibroblast growth factor-2. *Biochem Biophys Res Commun* **394**(3): 767–773.

Turner N, Grose R (2010) Fibroblast growth factor signalling: from development to cancer. *Nat Rev Cancer* **10**(2): 116–129.

Vasudev NS, Reynolds AR (2014) Anti-angiogenic therapy for cancer: current progress, unresolved questions and future directions. *Angiogenesis*; e-pub ahead of print 31 January 2014; doi:10.1007/s10456-014-9420-y.

Wang F, Kan M, Yan G, Xu J, McKeehan WL (1995) Alternately spliced NH2-terminal immunoglobulin-like Loop I in the ectodomain of the fibroblast growth factor (FGF) receptor 1 lowers affinity for both heparin and FGF-1. *J Biol Chem* **270**(17): 10231–10235.

Wang L, Park H, Chhim S, Ding Y, Jiang W, Queen C, Kim KJ (2012) A novel monoclonal antibody to fibroblast growth factor 2 effectively inhibits growth of hepatocellular carcinoma xenografts. *Mol Cancer Ther* **11**(4): 864–872.

Welti JC, Gourlaouen M, Powles T, Kudahetti SC, Wilson P, Berney DM, Reynolds AR (2011) Fibroblast growth factor 2 regulates endothelial cell sensitivity to sunitinib. *Oncogene* **30**(10): 1183–1193.

Workman P, Aboagye EO, Balkwill F, Balmain A, Bruder G, Chaplin DJ, Double JA, Everitt J, Farningham DA, Glennie MJ, Kelland LR, Robinson V, Stratford IJ, Tozer GM, Watson S, Wedge SR, Eccles SA. Committee of the National Cancer Research I (2010) Guidelines for the welfare and use of animals in cancer research. *Br J Cancer* **102**(11): 1555–1577.

Xue Y, Cao R, Nilsson D, Chen S, Westergren R, Hedlund EM, Martijn C, Rondahl L, Krauli P, Walum E, Enerback S, Cao Y (2008) FOXC2 controls Ang-2 expression and modulates angiogenesis, vascular patterning, remodeling, and functions in adipose tissue. *Proc Natl Acad Sci USA* **105**(29): 10167–10172.

Yen WC, Prudente RY, Corpuz MR, Negro-Vilar A, Lamph WW (2006) A selective retinoid X receptor agonist bexarotene (LGD1069, targretin) inhibits angiogenesis and metastasis in solid tumours. *Br J Cancer* **94**(5): 654–660.